Center for Turbulence Research
Proceedings of the Summer Program 1992

On the local nature of the energy cascade

By C. Meneveau[1], T. S. Lund[2] AND J. Chasnov[2]

The local nature of the energy cascade in space and time is studied using direct numerical simulation of decaying and forced isotropic turbulence. To examine the concept that large scales evolve into smaller ones, we compute the Lagrangian correlation coefficient between local kinetic energy at different scales. This correlation is found to peak at a Lagrangian time-delay that increases with scale separation. The results show that, on average, the flow of energy to smaller scales is predominantly local in physical space and that the view of eddies decaying into smaller ones while transferring their kinetic energy appears to be, on average, quite realistic. To examine the spectral characteristics of the cascade under unsteady conditions, a pulse of large-scale energy is added to the large-eddy simulation of forced isotropic turbulence. As time progresses, the evolution of this pulse through bands of increasing wavenumbers is studied.

1. Introduction

The theoretical framework underlying most turbulence modeling hypotheses is the Kolmogorov phenomenology, in which the cascade of energy from large to small scales occupies the central stage. It is postulated that the rate at which energy is dissipated is dictated by the large-scales and that the transfer of energy is mainly local in wave-number space. The $-5/3$ decay exponent in the inertial range, its extent, isotropy of small-scales, and so on, follow directly from these assumptions. This spatially averaged view is of importance for modeling at the Reynolds averaged level and is consistent with the 1941 version of Kolmogorov's theory. In the realm of sub-grid scale modeling for Large Eddy Simulations (LES), a slightly stronger version of the Kolmogorov phenomenology is at work. Spatial features of the energy cascade have to be taken into account, and the equilibrium between the *local* energy flux (or subgrid-scale energy production) and rate of dissipation is used to derive the popular Smagorinsky model. A spatially local version of the energy cascade is also invoked in models for small-scale intermittency (Kolmogorov, 1962; Meneveau & Sreenivasan 1991). In spite of the wide use of these ideas, the hypothesis that kinetic energy originally associated with some large-scale structure gets transferred to smaller flow structures that have evolved from the bigger one has never been directly tested. The purpose of the present work is to perform such an explicit test using direct numerical simulations. Several issues complicate this task. To properly account for the time needed for the energy transfer between scales as well as to take sweeping by the large scales properly into consideration, the flow structures

1 Johns Hopkins University
2 Center for Turbulence Research

have to be followed in time in a Lagrangian fashion. Also, proper statistical means have to be employed to ensure that the observed trends are robust. The calculation methods and results are presented in section 2.

The Kolmogorov phenomenology can also be used to make predictions about how the cascade should react to overall unsteadiness at the large scales. In a recent article, Lumley (1992) used the Kolmogorov phenomenology to predict that an energy pulse at largest scales will tend to 'propagate' along the spectrum, only to 'arrive' at small scales at some later time. This hypothesis is tested using simulations of forced isotropic turbulence. The results of these tests are reported in section 3. Conclusions are presented in Section 4.

2. Spatial structure of the energy cascade

Let the local kinetic energy of the flow-field composed of scales smaller than r', at location $\mathbf{x}$ and time t be denoted by $e_{r'}(\mathbf{x},t)$. As defined more precisely below, the effect of advection by scales larger than r' is excluded from $e_{r'}(\mathbf{x},t)$. Let us assume that at a certain instant and position this local energy is larger than the corresponding spatial average. The question we wish to address is how such a pulse will evolve in time if the underlying turbulent structure is followed as it is advected through space. The simplistic view of the energy cascade as consisting of large eddies breaking down to form smaller ones would suggest that if we follow a fluid element initially located at $(\mathbf{x},\mathbf{t})$ in a Lagrangian fashion, this pulse should become associated with local kinetic energy at decreasing scales as time progresses. In other words, we would expect that after following a fluid element with excess energy at scale r' for some time, we would find an excess of energy not at scale r', but at some smaller scale, say $r = r'/2$. To quantify such an effect statistically, it is useful to compute the correlation coefficient between local kinetic energies at different scales.

Several alternative definitions for the local kinetic energy will be used. The first is the trace of the subgrid-scale stress tensor (minus the Leonard term),

$$e_{r'}(\mathbf{x},t) = \widehat{u_k u_k} - \widehat{\widehat{u_k}\,\widehat{u_k}}. \tag{1}$$

The hat represents low-pass spatial filtering at scale r';

$$\widehat{a_{r'}}(\mathbf{x},t) \equiv \int a(\mathbf{x}',t) G_{r'}(\mathbf{x}-\mathbf{x}')d^3\mathbf{x}', \tag{2}$$

where $G_{r'}$ is a filter of characteristic scale r'. $e_{r'}(\mathbf{x},t)$ as defined according to Eq. (1) is the total kinetic energy minus the resolvable portion of the large scale kinetic energy. Decomposing the original velocity u_k into $u_k = \widehat{u_k} + u'_k$ shows that this definition also includes cross-terms of the form $\widehat{u'_k\widehat{u_k}}$. We shall also consider the kinetic energy of the small scales only, defined as

$$e_{r'}(\mathbf{x},t) = \widehat{u'_k u'_k}. \tag{3}$$

Notice that these definitions of local kinetic energy differ from the local wavelet spectrum (Meneveau, 1991) in the sense that they include the energy of all scales

smaller than the characteristic scale r' rather than just that of a particular spectral band.

The spatial filtering to be used can be of several forms. First, a spectral cut-off filter is considered, i.e.

$$G_{r'}(\mathbf{k}) = 1 \text{ if } |\mathbf{k}| < \frac{\pi}{r'}, \tag{4}$$

and zero otherwise. $G_{r'}(\mathbf{k})$ is the Fourier transform of $G_{r'}(\mathbf{x} - \mathbf{x}')$. We shall also consider Gaussian filter,

$$G_{r'}(\mathbf{x} - \mathbf{x}') = \left(\sqrt{\frac{6}{\pi}}\frac{1}{r'}\right)^3 \exp\left[-\frac{6(\mathbf{x} - \mathbf{x}')^2}{r'^2}\right], \tag{5}$$

and top-hat filter,

$$G_{r'}(\mathbf{x} - \mathbf{x}') = \frac{1}{r'} \text{ if } |\mathbf{x} - \mathbf{x}'| < \frac{r'}{2}. \tag{6}$$

At instant t_0, we compute the local energy at scale r', at some position $\mathbf{x}_0$. At later times, the local kinetic energy at a smaller scale $r < r'$ is computed at position displaced from $\mathbf{x}_0$ along the trajectory of a particle moving with velocity $\widetilde{u}_i$;

$$\mathbf{x} = \mathbf{x}_0 + \int_0^t \tilde{\mathbf{u}}(\mathbf{x}, t)dt, \tag{7}$$

where tilde now represents filtering at a smaller scale r. This posterior and smaller-scale local kinetic energy is defined either as

$$e_r(\mathbf{x}, t_0 + t) = \widetilde{u_k u_k} - \widetilde{\widetilde{u_k}\widetilde{u_k}}, \tag{8}$$

or as in Eq. (3), by replacing the filtering at scale r' (hat) by filtering at scale r (tilde).

Finally, the correlation coefficient between the two local kinetic energies depending on the Lagrangian time delay t and the scale ratio $b = r'/r$ is defined as

$$\rho(b, t) = \frac{< e_{br}(\mathbf{x}_0, t_0) e_r(\mathbf{x}, t_0 + t) > - < e_{br}(\mathbf{x}_0, t_0) >< e_r(\mathbf{x}, t_0 + t) >}{\sqrt{\sigma^2_{e_{br}} \sigma^2_{e_r}}}. \tag{9}$$

Here $\sigma^2_{e_{br}}$ and $\sigma^2_{e_r}$ are the variances of the local kinetic energies at scale br and r, respectively. Figure 1 illustrates the variables to be computed.

The correlation coefficient $\rho(b, t)$ will be used as a measure of how fluctuations of local energy propagate between different scales of motion as the underlying turbulent structures evolve in space and time. It can be measured for different definitions of local energy as well as different types of filters.

The next section describes the direct numerical simulations from which $\rho(b, t)$ is measured.

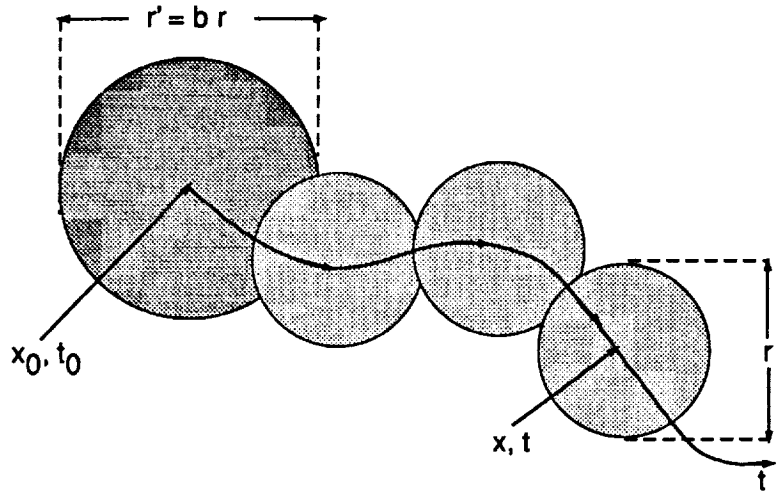

FIGURE 1. Sketch of local energy at 'large' scale $r' = br$, and at 'smaller' scale r after following a fluid particle for some time t.

2.1 Description of flow fields

Both forced and decaying isotropic turbulent fields were considered. They were generated with a pseudo-spectral code (Rogallo, 1981) on a 128 cubed mesh. The initial phases for the complex velocity field were chosen randomly but in such a way that the divergence-free condition was satisfied (see Rogallo, 1981 for more details on the initial conditions). Forcing was achieved by adding an anti-diffusion term (negative diffusion coefficient) to the Navier-stokes equations. The diffusion coefficient was wavenumber dependent and non-zero only for modes within wavenumber shells less than 3. The value of the coefficient for low wavenumbers was chosen so that the maximum wavenumber, scaled in Kolmogorov units, was unity (i.e. $k_{max}/\eta = 1$). To generate realistic steady-state turbulence, the flow was evolved for approximately 2 large scale eddy turn-over times. The Reynolds number, R_λ, settled at 95.8, while the velocity derivative skewness settled at -0.486. The energy spectrum is shown in Figure 2, where the vertical lines indicate the cut-off wavenumber at scale r (4 mesh spacings) and the maximum value of r', equal to $2.6r$. Note the tail-up in the energy spectrum at high wavenumbers. This results from the desire to achieve maximal Reynolds number for the given resolution. The dissipation range is not fully resolved, and, as a result, energy piles up there. It is generally believed (Rogallo, 1992) that the tail-up at high wavenumber will not adversely affect the data in the central portion of the spectrum used here. To generate data for the Lagrangian test, the simulation was run for approximately an additional 2 small scale eddy turnover times. In order to follow the evolution in time with sufficient accuracy, the entire velocity field was stored at 14 intermediate times, each separated by roughly 1/6th of the turn-over time associated with scales of size r (as estimated by $(\widetilde{S_{ij}}\widetilde{S_{ij}})^{-1/2}$).

For the decaying turbulence, the energy spectrum was initialized according to

$$E(k) = \frac{1}{32}\left(\frac{k}{2}\right)^4 \exp\left(-\frac{k}{2}\right). \tag{10}$$

This spectrum has its energy peak at wavenumber 8. In order to develop realistic turbulence from the random phase initial condition, the flow was allowed to evolve freely for 1.4 small scale eddy turnover times (based on quantities derived from the end of the initial run; $\tau_{t_0} = \frac{\lambda_0}{u'_0}$ where λ_0 and u'_0 are the Taylor microscale and the rms turbulence intensity, respectively). Over this period of time, the total turbulent kinetic energy decayed by 20%. The Taylor microscale Reynolds number $(u'\lambda/\nu)$ was 56.1. The 3-D radial energy spectrum at the end of this initial run is plotted in Kolmogorov units in Figure 3. Also shown are the experimental data of Comte-Bellot and Corrsin (1971), as well as two additional spectra for the later times t_6 and t_{13} discussed below. The simulation spectra collapse reasonably well with the experimental data for wavenumbers beyond the energy peak (where the universal scaling is expected to hold). As in the forced simulation, there is a noticeable energy pile-up at the highest wavenumbers.

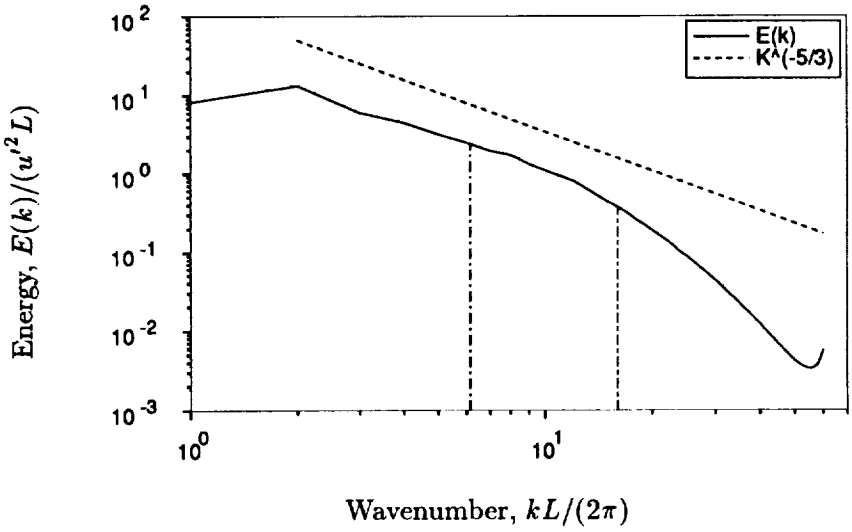

FIGURE 2. 3-D radial energy spectrum for the forced isotropic turbulence.

Data for the Lagrangian test was generated by evolving the flow approximately an additional two small scale eddy turn-over times, with 13 velocity fields saved at intervals of 1/6 of a turn-over time. Over this period of time, the kinetic energy decayed an additional 43%. The velocity derivative skewness changed from -0.382 to -0.302 in progressing from t_0 to t_{13}, while R_λ changed from 56.1 to 35.2. The vertical lines in Figure 3 correspond to the cut-off wavenumber of the scale r (4 mesh spacings in physical space) and the maximum $r' = 2.6r$ considered.

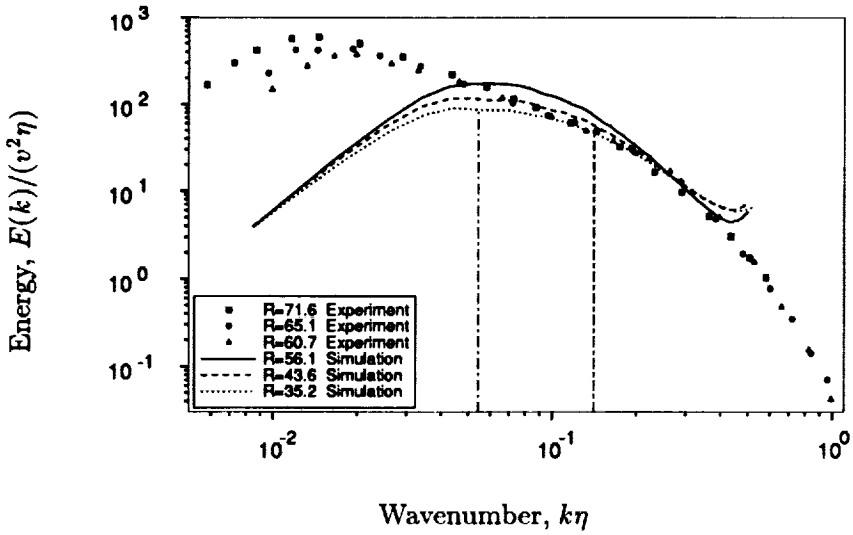

FIGURE 3. 3-D radial energy spectrum for the decaying isotropic turbulence, plotted in Kolmogorov units.

2.2 Calculations and results

The filtered velocity $\tilde{\mathbf{u}}$ was computed at scale r and sampled on a 32^3 mesh for each time t_0 to t_{13}. Also computed were the local energies e_{br} and e_r at every point of the coarse 32^3 mesh. For each grid-point on this mesh, Eq. (7) was integrated numerically using Euler's method with time increment $\Delta t = t_{n+1} - t_n$ and using multilinear interpolation to find the velocity between grid points. The local energy at $t = 0$ ($t_0 = 0$, say) of the larger scales (up to br) is computed for positions $\mathbf{x_0}$ corresponding to each grid point, and the final energy at scale r is obtained by multilinear interpolation of the field e_r at the end-points of the Lagrangian tracking, at all times t_1 to t_{13}. This calculation was repeated for different ratios $b = r'/r$ between the larger scale and smaller-scale energies, in a range $1 \leq b \leq 2.6$, where r is kept fixed and r' is increased.

First, we consider spectral cut-off filtering and the definition of local kinetic energy as the trace of the subgrid-scale tensor, according to Eq. (1). The results corresponding to the forced field are shown in Figure 4, and the results pertaining to the decaying field are shown in Figure 5. The time delay t has been normalized with the characteristic time-scale corresponding to the lower cut-off scale r at t_{13}:

$$|S| \equiv \sqrt{< \widetilde{S}_{ij} \widetilde{S}_{ij} >}. \qquad (11).$$

The upper curve corresponds to $b = 1$ and represents the Lagrangian autocorrelation function of the local kinetic energy. It exhibits the expected overall decorrelation time of the order of a few turn-over time scales of structures of size r.

The curves for $b > 1$, on the other hand, do not peak at $t = 0$, but at some later

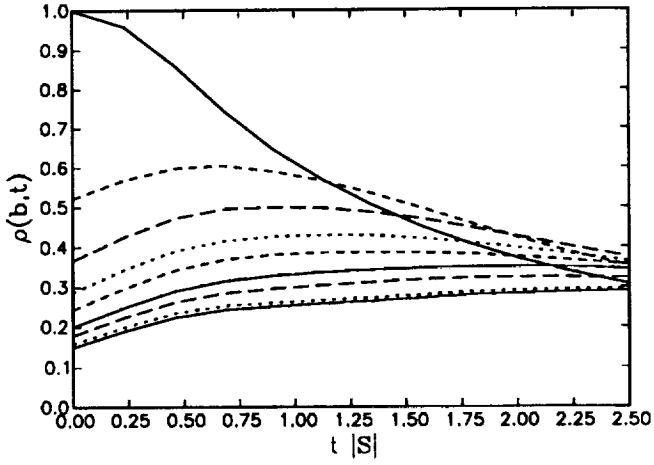

FIGURE 4. Correlation between local energies at different scales, as a function of Lagrangian time-delay. The flow is forced isotropic turbulence. The local energies are computed as the trace of the subgrid-scale stress tensor, using cut-off filtering. Different curves are for different scale separation; from top to bottom curve (at $t = 0$): $b = 1.0$,

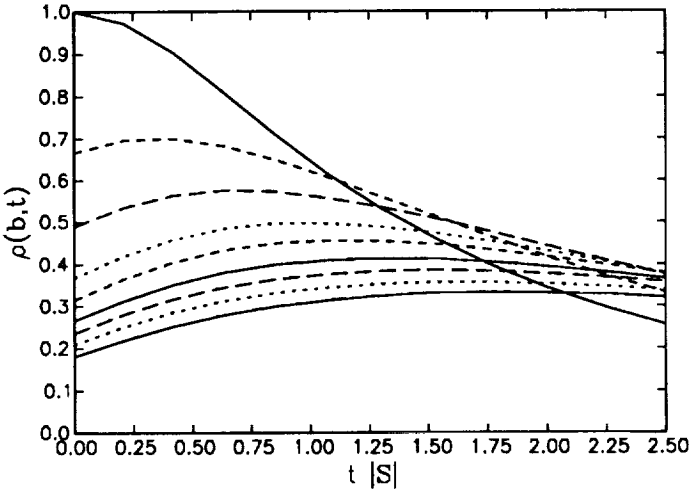

FIGURE 5. Same as Figure 4, but for the decaying isotropic turbulence simulation.

time. This time $(T_b)_{max}$ is an increasing function of the scale-ratio b. It implies that to exhibit maximum correlation between energy occurring at different scales some time must be allowed to pass. Pulses of higher local energy tend, on the average, to correlate better with pulses at smaller scales only after allowing the cascade to proceed for some time. As the ratio between scales becomes larger, this

time increases.

To verify that the approximate integration scheme to compute the Lagrangian path is sufficiently accurate for present purposes, the calculation is repeated using an even coarser resolution in time. This can be done by using every second field at t_0, t_2, t_4... t_{12}. The symbols in Figure 6 show the resulting correlation (for the forced flow, for $b = 1$, $b = 1.4$ and $b = 2$) as compared to the lines corresponding to the higher temporal resolution employing all fields t_0, t_1, t_2,.. etc. Only minor variations (less that 0.015 in the correlation coefficient) are visible, and we conclude that the procedure is sufficiently accurate.

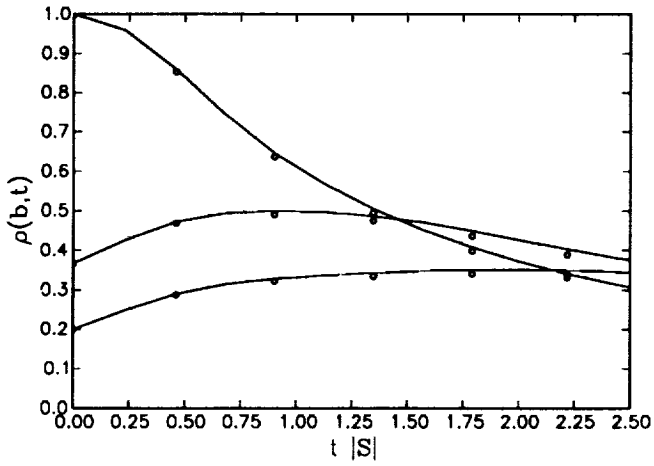

FIGURE 6. Test of sensitivity of results on accuracy of time integration, for the forced isotropic flow using the trace of the subgrid-scale tensor. Different solid curves are, from top to bottom: $b = 1$, 1.4, 2.0. The circles are obtained from a time-step that is twice as large, i.e. using every second of the stored fields only.

Next, we consider the second possible definition of local kinetic energy in terms of the product of small-scale velocities (Eq. (3)). Figure 7 shows the resulting correlations for the forced isotropic flow-field. The overall trend is the same as before, but the time at which the curves peak is slightly reduced.

The importance of different types of filtering is now quantified. Figures 8 and 9 show the correlation as a function of Lagrangian time for the Gaussian and top-hat filters. The local energy is now defined again according to Eq. (1). It is clear that considerable differences are present in terms of the peak time-delay as well as the magnitude of the correlation. Nevertheless, the basic trend of a time-delay that increases with scale separation is robust.

Finally, as an illustration of how the cascade of energy is associated with decreasing length-scales when following a fluid particle, we plot b^{-1} as a function of the peak time-delay $(T_b)_{max}$ in Figure 10. It contains all results pertaining to the cut-off filtering and the mean trend through the results pertaining to the Gaussian

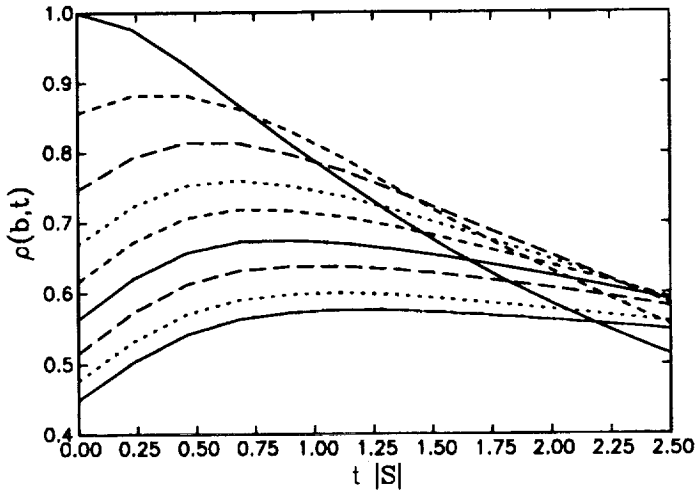

FIGURE 7. Same as Figure 4 but using Eq. to define local energy, and cut-off filtering applied to the forced isotropic flow.

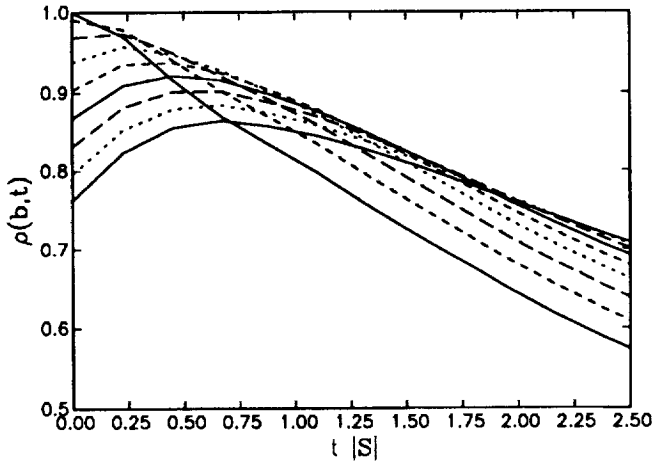

FIGURE 8. Same as Figure 4, but using a Gaussian filter.

and top-hat filter calculations. It can be seen that the data is consistent with a reduction in scale by a factor of 2, in a time that is of the order of $|S|^{-1}$.

Considerable scatter about this mean behavior is seen to exist. The largest variability is due to the filter type: The decrease in length-scale is considerably faster for the Gaussian or top-hat filter as compared to the spectral cut-off filter. The results for $b > 2.5$ are physically not very meaningful since the large-scale br already approaches the peak in the energy spectrum.

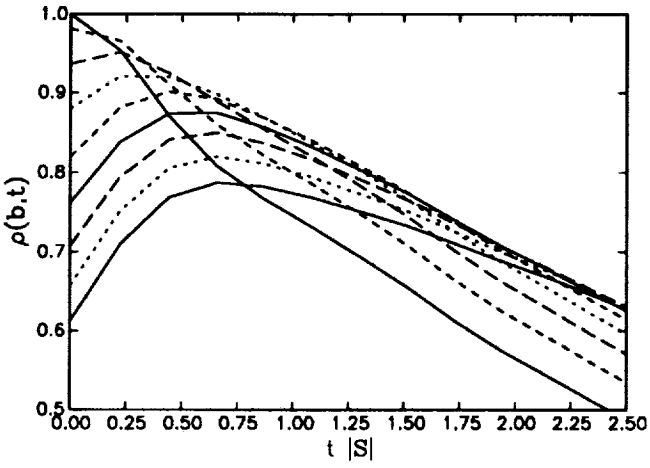

FIGURE 9. Same as Figure 4, but using a top-hat filter.

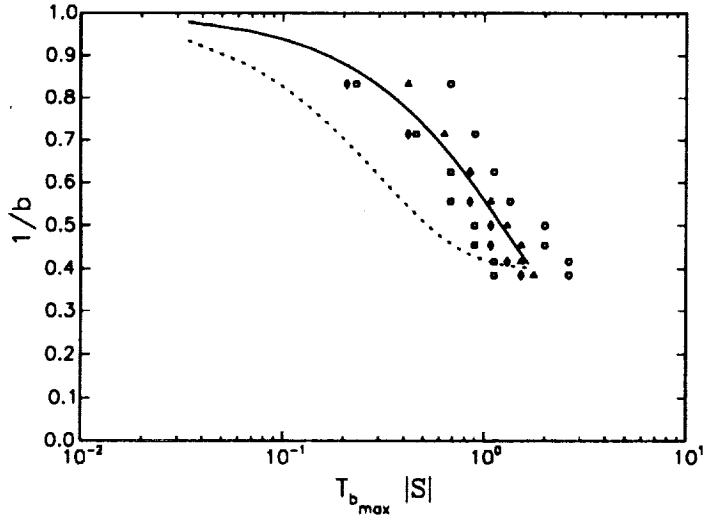

FIGURE 10. Plot of $1/b$ as a function of the corresponding time delay at which the two-point energy correlation peaks. It can be viewed as a decrease in length-scale of eddies as a function of time. Symbols are for the cut-off filtering. △ : decaying flow, local energy according to Eq. (1); ◇ : decaying flow, local energy according to Eq. (3); ○ : forced flow, local energy according to Eq. (1); □ : forced flow, local energy according to Eq. (3); ——— : mean trend through symbols; ---- : mean trend through all results corresponding to Gaussian and top-hat filtering.

3. Spectral evolution of sharp pulse of energy

In this section, we consider the temporal evolution of a sharp pulse of kinetic

energy originally present at low wavenumbers in the spectrum. To attain high Reynolds numbers, a large-eddy simulation was employed to study this case. We consider a high Reynolds number forced 128^3 LES using the subgrid-scale model described in Chasnov (1991). The method of forcing entails adjusting the energy of each Fourier mode in the first wavenumber shell $1 <= k < 2$ to a fixed value. The component distribution of the energy and the Fourier phases in the first shell evolve according to the Navier-Stokes equations. A long-time evolution of this forced flow together with the subgrid scale model results in an approximate $k^{-5/3}$ energy spectrum over the entire range of computational wavenumbers. The spectral subgrid-scale model used here contains both an eddy-viscosity and a stochastic backscatter term, that effects most strongly the evolution of modes closest to the cut-off wavenumber.

Starting from this fully-developed statistically-stationary inertial subrange, we have doubled the energy in the first band of wavenumbers at an initial time $t = 0$ by a simple rescaling of the Fourier amplitudes and followed the cascade of this energy to higher wavenumbers as a function of time. Figure 11 shows the results of this calculation. We plot the time-evolution of the energy in logarithmic bands of wavenumbers from the initial instant of time. The n^{th} band plotted represents the energy in the Fourier modes with wavenumbers between $2^{n-1} <= k < 2^n$. The energies are normalized by their values at $t = 0$. A plot of the energy in the first band would be a horizontal line at a value of two, and we expect that, for large-times, a statistically asymptotic state would develop where all the normalized energies approach a value of two.

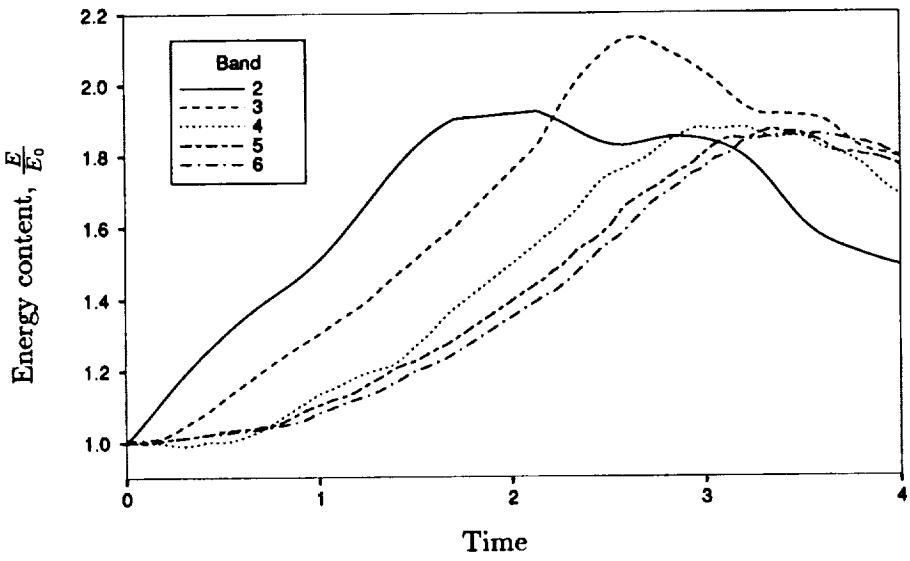

FIGURE 11. Time-evolution of the energy in logarithmic wavenumber bands after a pulse of energy was added to the first band. Band n represents the energy in wavenumbers $2^{n-1} <= k < 2^n$ normalized to its value at $t = 0$. Band 1 would be represented by a horizontal line at a value of 2.

There is evidently a large amount of statistical fluctuation in the data so that we limit ourselves to qualitative observations based on this single realization. A large eddy-turnover time based on the length of the computational box and the initial root-mean-square velocity may be computed and corresponds to approximately $t = 3$. The initial pulse of energy is, therefore, seen to become distributed more-or-less evenly among all the wavenumber bands on the order of a large-eddy turnover time. Furthermore, the cascade appears to proceed in a manner such that most of the energy is passed locally in wavespace (for $1 <= t <= 2$, the normalized energy level of the bands are ordered consecutively), but some of the energy is passed to all higher wavenumber bands (the normalized energy levels do not rise in a delayed step-like fashion, but rather begin to rise early on). Also, the time difference between consecutive peaks in Figure 11 is seen to decrease for the bands corresponding to larger wavenumbers, implying shorter turn-over times-cales for the smaller scales of motion.

These results are in qualitative agreement with the scenario described in Lumley (1992), where at each step in the energy cascade most of the energy is passed to the next higher wavenumber band while a diminishing fraction of the energy is passed to all other higher-wavenumber bands.

4. Summary and conclusions

First, it was shown that 'pulses' of kinetic energy of flow-structures at a particular scale will propagate to smaller scale structures as fluid particles are followed in time. This effect leads to a peak in the correlation between local energy at different scales occurring after a time delay. It was also shown that the time needed for a length-scale reduction factor of $b = 2$ is of the order of the 'characteristic' time scale in the energy cascade. Although these important qualitative results were very robust, quantitatively they were strongly dependent on filter type and on the precise definition used to compute the local energy density. Also, the increase in correlation after a Lagrangian time-delay was typically not very large. This is to be expected since the 'forward' flow of energy to smaller scales is itself a weak effect, coming from the difference between local forward flux and backscatter.

Secondly, unsteadiness in the large-scales of the flow were studied from the spectral point of view. A pulse of energy added at low wavenumbers in a high Reynolds number forced isotropic turbulence was observed to propagate to higher wavenumbers such that the energy levels increased faster in wavenumber bands closest to the initial pulse and slower in wavenumber bands farther away. The energy of the initial pulse was seen to be more-or-less evenly distributed among all the wavenumber bands in a time on the order of one large-eddy turnover time.

Acknowledgements

We thank P. Moin for stimulating discussions on this topic. This work was performed at the Center for Turbulence during the 1992 Summer Program. CM also acknowledges support from NSF CTS-9113048 and ONR N00014-92-J-1109.

REFERENCES

CHASNOV, J. R. 1991 Simulation of the Kolmogorov inertial subrange using an improved subgrid model. *Phys. Fluids A.* **3,** 188-200.

KOLMOGOROV A. N. 1941 Local structure of turbulence in an incompressible fluid at very high Reynolds number. *Dokl. AN SSSR.* **30,** 299

KOLMOGOROV A. N. 1962 A refinement of previous hypotheses concerning the local structure of turbulence in a viscous incompressible fluid at high Reynolds number. *J. Fluid Mech.* **13,** 82.

LUMLEY J. L. 1992 Some comments on turbulence. *Phys. Fluids A.* **4,** 203-211.

MENEVEAU C. 1991 Analysis of turbulence in the orthonormal wavelet representation. *J. Fluid Mech..* **232,** 469-520.

MENEVEAU C. & SREENIVASAN 1991 The multifractal nature of the turbulent energy dissipation. *J. Fluid Mech.* **224,** 429-484.

ROGALLO R. 1981 Numerical experiments in homogeneous turbulence. *NASA Tech. Mem.* 81315.

ROGALLO R. 1992 private communication.